Concentric Micromirror Array for High-Speed Optical Dynamic Focusing

Nathan Tessema Ersumo[1,2], Cem Yalcin[2], Nicolas Pégard[3], Laura Waller[2,4], Daniel Lopez[5], and Rikky Muller[1,2,4]

[1] University of California, Berkeley - University of California, San Francisco Graduate Program in Bioengineering, USA

[2] Departement of Electrical Engineering & Computer Sciences, University of California, Berkeley, CA 94720, USA

[3] Department of Applied Physical Sciences, University of North Carolina at Chapel Hill, Chapel Hill, NC 27514, USA.

[4] Chan Zuckerberg Biohub, San Francisco, CA 94158, USA

[5] Center for Nanoscale Materials, Argonne National Laboratory, Argonne, IL 60439, USA

***Abstract*— Optical dynamic focusing has emerged as a speed, complexity and efficiency bottleneck across various applications, which include scanning multi-photon microscopy in biology, maskless lithography and micro-machining in material processing, and wavefront correction. Here, we present a 32-ring 23,852-pixel concentric micromirror array capable of performing dynamic focusing for wavelengths of up to 1040 nm with a response rate of up to 8.75 kHz, 30 V drive and a focusing full-width-half-maximum to range ratio of 4.8%.**

Keywords—MEMS, micromirror, dynamic focusing, varifocal, high-speed

I. Introduction

The capacity to rapidly sculpt light in 3 dimensions is vital to the performance of various techniques in biology (ex: 3D multi-photon microscopy) [1], fabrication (ex: maskless lithography [2] and laser micro-machining [3]) and high-speed adaptive optics [4]. Though tools such as galvanometer scan mirrors and acousto-optic deflectors (AODs) are capable of lateral steering refresh rates of tens of kHz [1], [5], dynamic axial focusing remains a bottleneck limiting data throughput. The most widely used embodiment of focus tuning today employs electrically shape changing lenses with refresh rates of under 20 Hz [1]. Alternative technologies, including electro-optic lenses [5], tunable acoustic gradient index of refraction lenses [6], and cascaded AODs [7], can reach refresh rates of 1 MHz. But since they are each hindered by fundamental limitations, namely lack of dwelling capacity, high voltage requirements (~300 V) and low efficiency (10-50%) respectively, the development of a suitable general-purpose device for this application remains elusive.

To enable high-speed dynamic focusing, a tool should (a) be agnostic to polarization and wavelength, (b) achieve low settling time and high dwell time, and (c) be robust against insertion complexity and loss. Capacitively transduced piston-type micromirrors are an attractive building block [2] for dynamic focusing since they can be used to introduce and maintain a desired phase shift profile on any incident light by changing local optical path lengths at settling times as low as 20 µs through simple open-loop voltage drive. Accordingly, a piston-motion micromirror array-based dynamic focusing system is presented here. The working principle of the device is shown in Fig. 1 a-b. The array forms a series of concentric rings (Fig. 1c) that effectively amount to a mirror surface with adjustable radial curvature. Structural stability is ensured by partitioning the rings into an array of square micromirrors (or pixels), as shown in Fig. 1d.

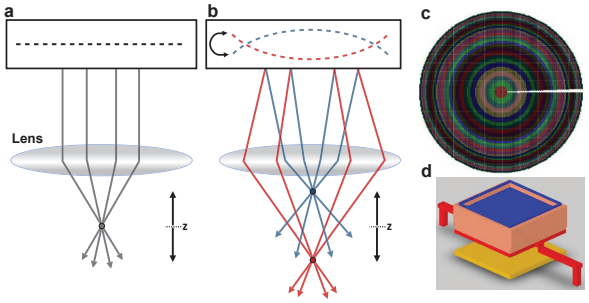

Fig. 1. a-b: Principle of operation for z-axis focusing with accompanying lens (a) with and (b) without array actuation. c: Full micro-mirror array. d: Pixel-level structure.

II. Design and Fabrication

Micromirror behavior was simulated using analytical and finite element models to determine performance metrics as a function of parameters relating to geometry and residual stress. With these models, we determined the dimensional specifications required for a displacement range exceeding 500 nm for operation with wavelengths extending up to the infrared domain, and a full-scale driving voltage range of under 30 V.

The micromirror array was designed for and fabricated under the MEMSCAP Poly-MUMPs® service with custom thickness modification and post-processing metallization via evaporation and lift-off. With a pitch of 48 µm, each pixel consists of a fixed bottom electrode for voltage drive, two gap stops, and two clamped-guided beams suspending an electrically grounded 40 µm wide mirror body formed by a reinforced stack of two polysilicon layers and a reflective gold surface. The entire 23,852-pixel array has a radius of 4.1 mm and is comprised of 32 independently actuated rings with varying track widths to account for the radial slope of parabolic surfaces. A 7.2° radial slice was reserved for wiring to bond pads. Fabricated array images are shown in Fig. 2.

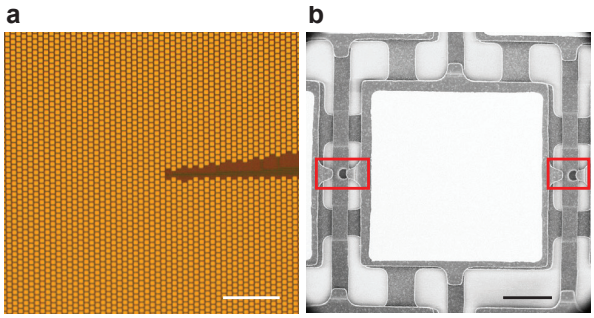

Fig. 2. a: Microscopy image of array (Scale bar: 100 µm). b: Scanning electron microscopy image of pixel (Scale bar: 10 µm). Gap stop structures are demarcated by red boxes.

978-1-7281-4503-7/19/$31.00 ©2019 IEEE

III. Performance

The micromirror array was driven using an ADI AD5535B 32-channel DAC, an Opal Kelly XEM6010-LX150 FPGA, and custom firmware and software. For pixel-level performance characterization, a Lyncée Tec Digital Holographic Microscope (DHM®-R1000) was used to measure vertical static displacement Δx vs. applied voltage V behavior as shown in Fig. 3a. Fitting to the general form of the analytical solution to parallel plate transduction, $V = \sqrt{ax(b-\Delta x)^2}$ where b is a measure of electrode gap distance, was performed, and the adjusted R^2 value for all fits was greater than 0.999. For the average static voltage response curve, b was found to be 2160 nm, which is close to the nominal designed value of 2000 nm, and 540 nm of displacement was reached with a 29.6 V drive. Gap stops placed at a travel distance of 750 nm were also found to be effective in preventing shorting from pull-in. To measure mirror response time as shown in Fig. 3b, a stroboscopic unit was used in conjunction with the DHM to apply a 1 kHz square wave driving signal while sampling was performed at 100 kHz. The average 2% settling time was found to be 114 µs.

Full array performance was evaluated by first measuring inter-pixel and intra-pixel height variations across numerous pixels from different rings with and without actuation using the DHM and atomic force microscopy. These height variation distributions reflecting geometric and process non-idealities were subsequently computationally introduced to ideal phase masks corresponding to a range of target defocus depths. Finally, using these empirically generated expected phase profiles, propagation of the reflected wave was simulated with a custom 3D optical simulation framework as shown in Fig. 4. The incident light was set to be a 1040 nm wavelength Gaussian beam and the focal length of the accompanying lens was set to 0.2 m. The operating range, i.e. the range across which on-axis peak intensity of the defocused spot exceeds maximum diffractive noise intensity, was found to be 230 mm while the z-axis full width at half maximum (FWHM) of the spot was measured to be 11 mm. Accordingly, the FWHM-to-range ratio, which is indicative of magnification-independent defocusing performance and corresponds to the percentage of the operating range that a defocused light spot represents, was assessed to be 4.8%.

Conclusion

We demonstrate the successful design and implementation of a dynamic focusing micromirror array for wavelengths of up to 1040 nm, with 30 V drive, and with a full width at half maximum to range ratio of 4.8%. The array's 8.75 kHz response rate, which was achieved without compromising polarization independence, ease of operation, dwell time and efficiency, is two orders of magnitude greater than that of existing general-purpose commercial tools. This improvement brings dynamic axial focusing in line with speeds seen in state of the art lateral scanning tools, eliminating the throughput bottleneck in viable joint integration setups for optical 3D scanning. Metasurface patterning on top of these micromirrors can also be envisioned for synergistic enhancement of capability [8].

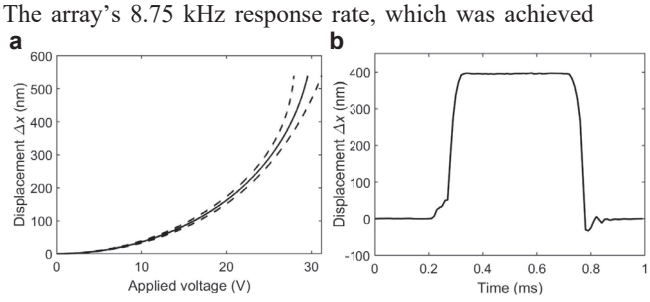

Fig. 3. a: Average displacement vs. voltage curve ± standard deviation. From fit: a=6.167x10^{-7} V^2/nm^3 and b=2160 nm. b: Dynamic response to 20-30 V step.

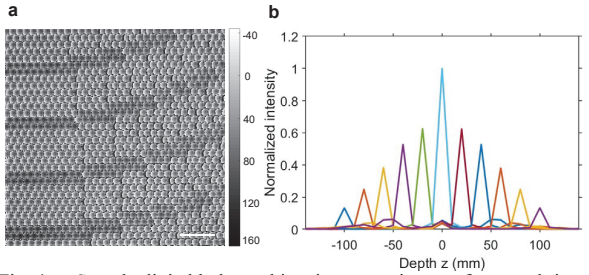

Fig. 4. a: Sample digital holographic microscopy image of actuated rings (vertical colorbar in nm, scale bar is 100 µm). b. Defocusing performance simulation using measured inter-pixel and intra-pixel height variation information: on-axis normalized intensity across depth is plotted in different colors for array-level phase profiles corresponding to target defocusing depths across the entire operating range. Depth z of 0 corresponds to rear focal plane of accompanying lens.

Acknowledgment

The authors thank Prof. Ming Wu, the Marvell Nanofabrication Laboratory, Dr. Soner Sonmezoglu, and Analog Devices for tools and guidance. This work was performed, in part, at the Center for Nanoscale Materials, a U.S. Department of Energy Office of Science User Facility, and supported by the U.S. Department of Energy, Office of Science, under Contract No. DE-AC02-06CH11357.

References

[1] M. dal Maschio, J. C. Donovan, T. O. Helmbrecht, and H. Baier, "Linking Neurons to Network Function and Behavior by Two-Photon Holographic Optogenetics and Volumetric Imaging," *Neuron*, vol. 94, no. 4, p. 774–789.e5, May 2017.

[2] G. P. Watson et al., "Spatial light modulator for maskless optical projection lithography," *J. Vac. Sci. Technol. B Microelectron. Nanom. Struct. Process. Meas. Phenom.*, vol. 24, no. 6, pp. 2852–2856, Nov. 2006.

[3] T.-H. Chen, R. Fardel, and C. B. Arnold, "Ultrafast z-scanning for high-efficiency laser micro-machining," *Light Sci. Appl.*, vol. 7, no. 4, p. 17181, Apr. 2018.

[4] Y. Yu, T. Zhang, A. Meadway, X. Wang, and Y. Zhang, "High-speed adaptive optics for imaging of the living human eye," *Opt. Express*, vol. 23, no. 18, p. 23035, Sep. 2015.

[5] J. Heberle, P. Bechtold, J. Strauß, and M. Schmidt, "Electro-optic and acousto-optic laser beam scanners," in *Laser-based Micro- and Nanoprocessing X*, 2016, vol. 9736, p. 97360L.

[6] C. B. Arnold, C. Theriault, D. Amrhein, S. Kang, and E. Dotsenko, "Ultra-high-speed variable focus optics for novel applications in advanced imaging," in *Photonic Instrumentation Engineering V*, 2018, vol. 10539, p. 1.

[7] G. D. Reddy and P. Saggau, "Fast three-dimensional laser scanning scheme using acousto-optic deflectors," *J. Biomed. Opt.*, vol. 10, no. 6, p. 064038, 2005.

[8] Roy, T., Zhang, S., Jung, I.W., Troccoli, M., Capasso, F. and Lopez, D. "Dynamic metasurface lens based on MEMS technology". *Apl Photonics*, *3*(2), p.021302, 2018.